



Low frequency vibration tests on a floating slab track in an underground laboratory*

De-yun DING^{†1,2}, Wei-ning LIU¹, Ke-fei LI¹, Xiao-jing SUN¹, Wei-feng LIU¹

(¹School of Civil Engineering, Beijing Jiaotong University, Beijing 100044, China)

(²Beijing Urban Engineering Design and Research Institute Co., Ltd., Beijing 100037, China)

[†]E-mail: dyding2301@163.com

Received June 9, 2010; Revision accepted Dec. 21, 2010; Crosschecked Apr. 24, 2011

Abstract: Low frequency vibrations induced by underground railways have attracted increasing attention in recent years. To obtain the characteristics of low frequency vibrations and the low frequency performance of a floating slab track (FST), low frequency vibration tests on an FST in an underground laboratory at Beijing Jiaotong University were carried out. The FST and an unbalanced shaker SBZ30 for dynamic simulation were designed for use in low frequency vibration experiments. Vibration measurements were performed on the bogie of the unbalanced shaker, the rail, the slab, the tunnel invert, the tunnel wall, the tunnel apex, and on the ground surface at distances varying from 0 to 80 m from the track. Measurements were also made on several floors of an adjacent building. Detailed results of low frequency vibration tests were reported. The attenuation of low frequency vibrations with the distance from the track was presented, as well as the responses of different floors of the building. The experimental results could be regarded as a reference for developing methods to control low frequency vibrations and for adopting countermeasures.

Key words: Low frequency vibrations, Laboratory tests, Floating slab track (FST), Vibration isolation efficiency

doi:10.1631/jzus.A1000276

Document code: A

CLC number: U231+2

1 Introduction

With the rapid development of urban rail transit systems, some underground railway lines may pass through vibration-sensitive zones such as scientific research facilities, universities, hospitals, and precision manufacturing factories. For instance, Beijing Metro Lines 4, 8, 10, and 15 pass through the Physics Laboratory of Beijing University, the National Measurement Laboratory, the China Academy of Space Technology, and Tsinghua University, respectively, where a lot of equipment used for scientific research is highly sensitive to environmental vibrations, in particular, potential low frequency vibrations of less than 15 Hz,

which have become a special concern (Liu *et al.*, 2005b; Liu *et al.*, 2006; Gupta *et al.*, 2008; Ding *et al.*, 2008b; 2009; 2010).

In-situ measurements are undoubtedly the most useful data for evaluating vibrations induced by underground railways. The earliest measurements of metro-induced vibrations were obtained from the Berlin Metro (Ruker, 1977). Vibration at Baker Street on the Jubilee Line of the London Underground was measured (London Transport Office of the Scientific Adviser, 1982). Measurements were collected from a running tunnel of the Beijing subway to obtain the dynamic response at specified points on the tunnel lining (Pan and Xie, 1990). Ground vibrations induced by underground light rail transit (LRT) operations were measured to predict low frequency ground vibration (Wolf, 2003). Vibration measurements in the running tunnel and on the ground surface were obtained from the Dongdan-Jianguomen Section of

* Project supported by the National Natural Science Foundation of China (No. 51008017), and the Fundamental Research Funds for the Central Universities of China (Nos. 2009JBM074 and 2009JBM075)
 © Zhejiang University and Springer-Verlag Berlin Heidelberg 2011

Line 1 of the Beijing Metro to obtain the characteristics of vibrations due to metro trains (Liu *et al.*, 2005a). A number of vibration measurements from the different track forms used on the bay area rapid transit (BART) system were obtained (Saurenman and Phillips, 2006). In-situ vibration measurements were collected as part of the CONVURT project at a site in Regent's Park on the Bakerloo Line of the London Underground during 35 passages of a test train at a speed of between 20 and 50 km/h (Degrande *et al.*, 2006). All these studies concentrated mainly on practical underground railways in operation.

Various countermeasures were developed to control the problem of vibrations from underground trains. A floating slab track (FST) called the mass-spring system is a typical vibration isolation measure, which has been applied widely in underground railways to mitigate vibrations (Wilson *et al.*, 1983; Nelson, 1996; Cui and Chew, 2000; Zhang and Xu, 2002; Sun *et al.*, 2005; Lombaert *et al.*, 2006; Kuo *et al.*, 2008). An FST can isolate vibration levels up to 40 dB, and its basic frequency is usually less than 15 Hz. There are two kinds of FSTs depending on the type of support: rubber bearing and steel spring. Generally, the basic frequency of a steel spring FST is lower than that of a rubber bearing FST.

Based on the low basic frequency and effective isolation performance of FSTs, Beijing Jiaotong University (BJTU) designed a steel spring FST, and conducted low frequency vibration tests in the Lab of Track Vibration Abatement and Control (LTVAC) on the campus, to attempt to determine the characteristics of the low frequency vibrations and the low frequency performance of the steel spring FST.

The main objective of this paper was to describe the results of low frequency vibration tests on the steel spring FST under different supporting conditions. The responses from the track, the tunnel, the ground surface, and the vicinity of the building were obtained. A law of low frequency vibration attenuation with distance from the track was presented, and the low frequency vibrations as a function of the floor number of the building were outlined.

2 Low frequency vibration tests

Low frequency vibration measurements were obtained from the tunnel, the ground surface, and the

building sites (Fig. 1). The LTVAC is located in the southeastern part of the BJTU campus, and is surrounded by the Laboratory of All-optical Network and Modern Communications Network to the northeast, a construction zone to the northwest, and the Tunnel Center Building to the south. The Tunnel Center Building is a reinforced concrete frame structure supported by a strip foundation, and it consists of a laboratory and an office building. The part of the structure close to the LTVAC is a laboratory with a height of 6 m, and the rest is a four-floor 12-meter-tall office building.

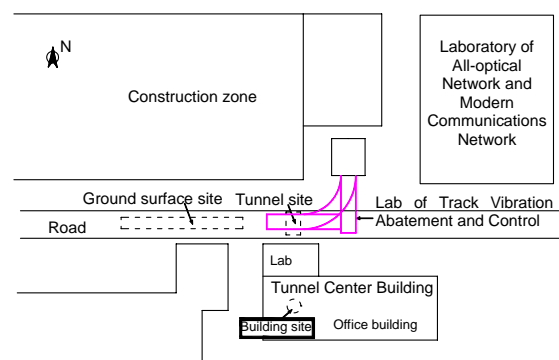


Fig. 1 Plan of the measurement sites on the campus of Beijing Jiaotong University

2.1 Characteristics of the laboratory

The LTVAC has two floors, 1 and 2 (Fig. 2). Floor 1 is a curved tunnel with a small radius of 12.5 m, embedded in sandy silt to a depth of 6 m below ground. Floor 2 is an L-type tunnel, inserted in gravel to a depth of 14 m, a substrate similar to that of the underground railway in Beijing. Both tunnels have the same type of upright-wall concrete lining with a thickness of 0.55 m. The clear width and height of each tunnel are both 4 m.

2.2 Characteristics of the floating slab track

The FST was mounted on the invert of floor 2 at a distance of 3.8 m from the tunnel end to the middle cross section (Fig. 2). It was supported by two rows of steel springs installed in holes. The stiffness of the springs was either 6.9×10^6 or 5.3×10^6 N/m, and they were spaced at intervals of 1.2, 1.8 or 2.4 m (Fig. 3).

The length, width, and thickness of the slab were 6, 3.5, and 0.45 m, respectively, and the mass of the slab M_{slab} was 22 680 kg. T-60 rails with a mass per unit length of 60.64 kg/m were used, and their total

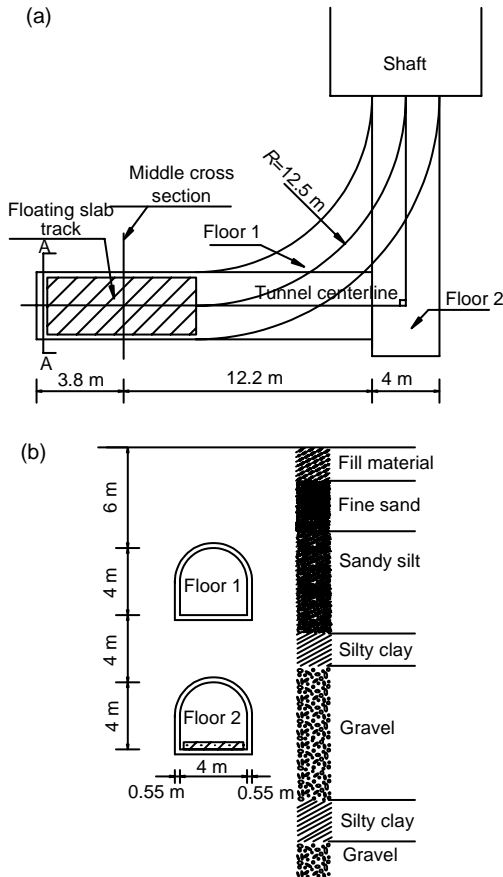


Fig. 2 Laboratory of Track Vibration Abatement and Control

(a) Plan; (b) A-A cross section. *R*: radius of tunnel

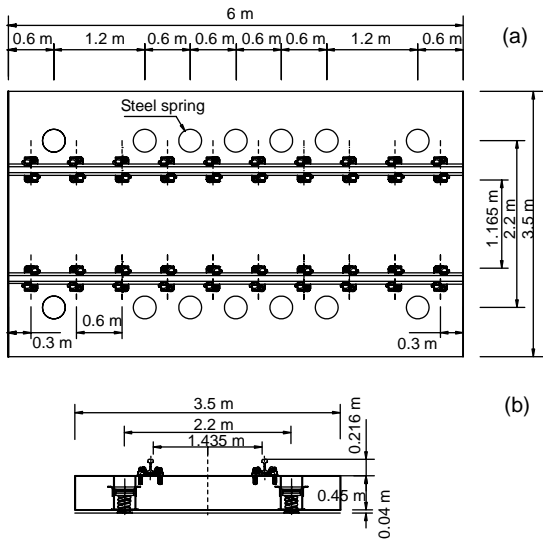


Fig. 3 Plan (a) and cross section (b) of floating slab track

mass M_{rail} is 728 kg. Rubber rail pads with a stiffness of 5.0×10^7 N/m discretely supported the rails at intervals of 0.6 m on the slab.

2.3 Unbalanced shaker SBZ30

To simulate train induced vibrations, an unbalanced shaker SBZ30 for dynamic simulation (Fig. 4) was made, with a total mass $M_{shaker}=18400$ kg. It consisted of a vibration generator and a bogie. The vibration generator had a static eccentric moment in the range of 0 to 250 N·m, and the rotation speed of the eccentric axis was between 0 and 1800 r/min. The unbalanced shaker could produce harmonic loads with amplitudes ranging from 0 to 2.5×10^5 N within the frequency range between 5 and 30 Hz. The distance between the two pairs of wheels was 2.2 m, which was similar to that of a Beijing metro train.



Fig. 4 Unbalanced shaker SBZ30 used for the dynamic simulation

2.4 Test cases

According to the stiffness, spacing, and allowable deformation of the steel springs, some test cases were designed (Table 1). Case 1 was regarded as a non-isolation measure without the springs installed between the slab and the tunnel invert; Cases 2, 3, 4, and 5 were considered as the isolation measures.

For Cases 2, 3, 4, and 5, four kinds of steel spring combinations were used with four kinds of total effective spring stiffness $K_{case_i}=6.9 \times 10^7$, 5.3×10^7 , 5.52×10^7 , and 4.14×10^7 N/m, respectively. The basic frequencies of the cases with isolation measures could be calculated approximately using the formula $f_{case_i}=[K_{case_i}/(M_{slab}+M_{rail})]^{1/2}/(2\pi)$, resulting in $f_{case_i}=8.65$, 7.58, 7.73, and 6.70 Hz, respectively. These frequencies were slightly different from those of 8.12, 7.12, 7.31, and 6.50 Hz calculated using the 3D finite

element method based on the theory of multiple-degree-of-freedom systems (Ding *et al.*, 2008a). If the unbalanced shaker SBZ30 was considered to contribute to the vibration of the track, the basic frequencies would be changed by the formula $f_{case_i}=[K_{case_i}/(M_{slab}+M_{rail}+M_{shaker})]^{1/2}/(2\pi)$, resulting in $f_{case_i}=6.47, 5.67, 5.79, 5.01$ Hz. The basic frequency in Case 3 was similar to that of Case 4; however, the spacing and allowable deformation of steel springs were different between Case 3 and Case 4. For all cases, the effect of differences between the non-isolation and isolation measures on the dynamic characteristics of the FST could be compared, as well as the influence of different sizes of stiffness and spacing of the steel springs.

For all cases, harmonic excitation forces ($1.1 \times 10^4, 1.46 \times 10^4, 1.99 \times 10^4, 2.59 \times 10^4, 3.28 \times 10^4, 4.05 \times 10^4, 4.90 \times 10^4, 5.83 \times 10^4, 6.84 \times 10^4, 7.94 \times 10^4, 9.11 \times 10^4, 1.0 \times 10^5$ N) produced by the unbalanced shaker SBZ30 between 5.2 and 16 Hz (5.2, 6, 7, 8, 9, 10, 11, 12, 13, 14, 15, 16 Hz) were adopted, based on the research objective and the work requirement of the unbalanced shaker. The maximum force F_{max} was 1.0×10^5 N, and therefore the corresponding maximum deformation of the steel springs could be obtained by $D_{case_i}=[(M_{slab}+M_{rail}+M_{shaker})g+F_{max}]/K_{case_i}$, resulting in $D_{case_i}=7.4, 9.6, 9.2, 12.3$ mm, which indicated that the deformations of the steel springs were within the allowable range (Table 1).

Table 1 Test cases

No. ¹	Stiffness ($\times 10^6, \text{N/m}$)	Spacing*	D_{all} (mm)	No. ²	Spring location**
1		Non-isolation			
2	6.9	1.2 m \times 4	15	10	••••••••
3	5.3	1.2 m \times 4	10	10	••••••••
4	6.9	1.8, 1.8, 1.2 m	15	8	••••••••
5	6.9	2.4 m \times 2	15	6	••••••••

¹ Case number; ² Spring number; * Spacings are vertically symmetrical distributed, and only a half has been presented, i.e., 1.2 m \times 4 means four spacings of 1.2 m each between every two springs in the upper half; ** Sketch of spring location (black filled circle); D_{all} : allowable deformation

2.5 Experimental setup

A right-handed Cartesian frame of reference was defined with the origin at the tunnel invert on the middle cross section, the x -axis perpendicular to the

tunnel centerline, the longitudinal y -axis in the direction of the tunnel centerline, and the z -axis pointing upwards. Vertical accelerations in the tunnel were measured at six different points, T1, T2, T3, T4, T5, and T6, in the $y=0$ plane (Fig. 5a). As shown in Figs. 5b–5g, six Lance accelerometers were glued to the bogie, rail, slab, tunnel invert, tunnel wall, and tunnel apex, respectively. The sensitivity of each accelerometer was 250 m·V/g in the frequency range

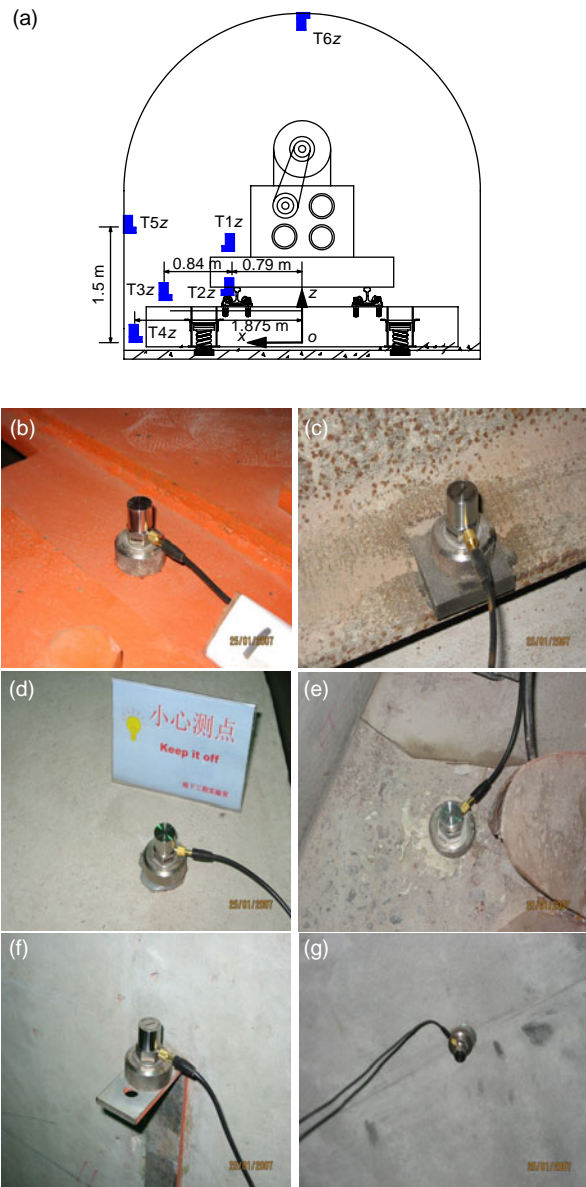


Fig. 5 Measurement setup in the tunnel

(a) Cross section of measurement points; (b) T1 on the bogie; (c) T2 on the rail; (d) T3 on the slab; (e) T4 on the tunnel invert; (f) T5 on the tunnel wall; (g) T6 on the tunnel apex

between 0.35 and 6000 Hz, and its measurement range was 20 g. The vibration signals were recorded using Wavebook 516E data acquisition with 8 channels at a sampling rate of 512 Hz.

Vertical and horizontal (in the y -direction) accelerations were measured at five points, S1, S2, S3, S4, and S5, located on the ground surface (Fig. 6a). Ten Lance accelerometers with a high sensitivity of 40 V/g in the frequency range between 0.2 and 600 Hz and a measurement range of 0.125 g were placed at horizontal distances of 0, 20, 40, 60, and 80 m from the middle cross section. At each point, two accelerometers were mounted on a rectangle steel saddle (Fig. 6b). A FOCUS II dynamic data acquisition analysis apparatus with 8 channels was used to record the vibration signals at a sampling frequency of 512 Hz.

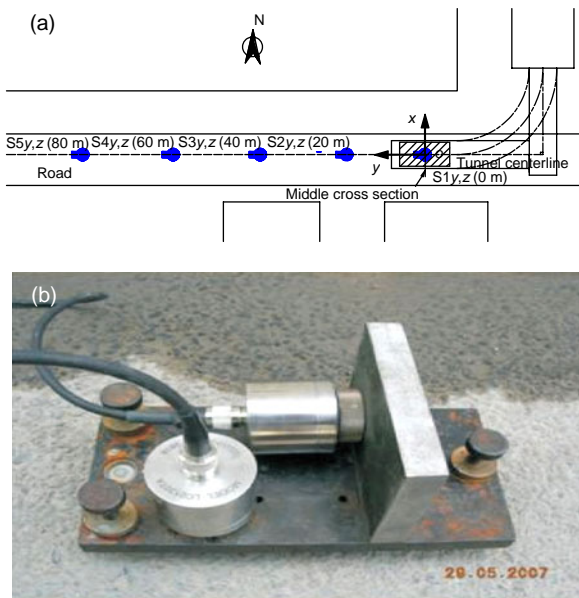


Fig. 6 Measurement setup on the ground surface

(a) Plan of measurement points; (b) Accelerometers mounted on a rectangular steel saddle

Fig. 7 shows the location of the measurement points B1, B2, B3, and B4 in the Tunnel Center Building and accelerometers placed on the first floor. On each floor, vertical and horizontal (in the x -direction) accelerations were measured in the corridor at a horizontal distance of 23 m from the tunnel centerline in the $y=0$ plane. The same accelerometers and data acquisition analysis apparatus were used as on the ground surface.

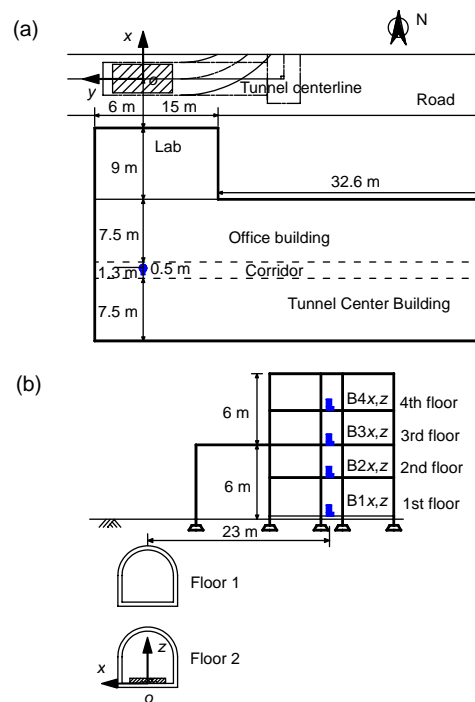


Fig. 7 Measurement setup in the building

(a) Plan of measurement points; (b) Cross section of measurement points; (c) Accelerometers placed on the 1st floor

3 Analysis of test data

3.1 Data processing

The magnitude of excitation forces varied from 1.1×10^4 to 1.0×10^5 N in the frequency range between 5.2 and 16 Hz. To obtain comparable results, the assumption that excitation force varied directly with vibration acceleration was used in data processing, based on the small deformation of elasticity theory. Therefore, the recorded accelerations could be normalized into unit-force accelerations. Note that the unit force was equal to 1.0×10^3 N. In the following data analysis, the normalized accelerations were adopted.

The vibration acceleration level (VAL, dB), vibration transfer loss (VTL, dB), insertion loss (IL, dB) and transmission coefficient (TC) are expressed as follows:

$$VAL = 20\lg(a / a_0), \tag{1}$$

$$VTL = VAL_i - VAL_k, \tag{2}$$

$$IL = 20\lg(a_{uniso} / a_{iso}), \tag{3}$$

$$TC = \frac{\frac{1}{2\pi} \int_{-\infty}^{+\infty} Y(t) \exp(-j2\pi ft) dt}{\frac{1}{2\pi} \int_{-\infty}^{+\infty} X(t) \exp(-j2\pi ft) dt} = \frac{Y(f)}{X(f)}, \tag{4}$$

where a is the root mean square (RMS) of vibration acceleration, and $a_0=10^{-6} \text{ m/s}^2$ is the reference vibration acceleration; subscripts 'i' and 'k' refer to different positions, while 'uniso' and 'iso' refer to the non-isolation and isolation measures, respectively; $X(t)$ and $Y(t)$ are the input and output respectively of the vibration system, $X(f)$ and $Y(f)$ are the input and output Fourier transformations respectively of the vibration system, t is the time, and f is the frequency.

3.2 Responses of the track and the tunnel

In the following analysis of vibration responses from different cases, Case 3 is omitted, because the response was almost the same as that of Case 4.

Fig. 8 summarizes the vertical VALs at different positions in the tunnel in different cases. In every case, the trends at different positions were similar. In Case 1, the vertical VAL reached a maximum at around 12 Hz, which can be explained by the resonance of the unbalanced shaker SBZ30. There was a marked peak at about 7 Hz in Case 2, and peaks occurred around 6 Hz in Cases 4 and 5, explained by the resonance of the whole system including the FST and the unbalanced shaker SBZ30. It can be clearly seen that the resonance frequency shifted from 12 to 6 or 7 Hz with the installation of steel springs. Note that the resonance frequencies seem somewhat different from the basic frequencies in Section 2.4, because the interfaces between the FST and the unbalanced shaker were not rigid during the vibration tests.

The vertical VALs on the bogie (T1), rail (T2), and slab (T3) were obviously larger than those on the tunnel invert (T4), tunnel wall (T5), and tunnel

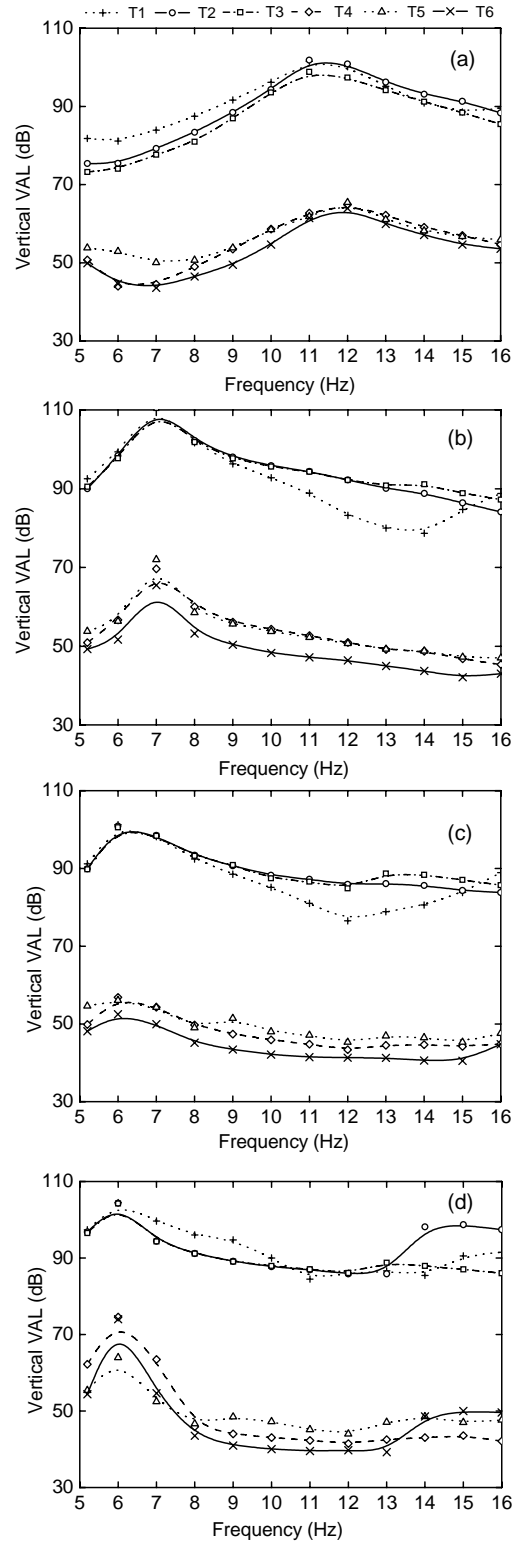


Fig. 8 Vertical vibration acceleration levels (VALs) at different positions in the tunnel in different cases (a) Case 1; (b) Case 2; (c) Case 4; (d) Case 5

apex (T6). The VTL from the slab to the tunnel invert attenuated in the range between 29.7 and 46.2 dB, according to the statistic of the vertical VALs at different positions in different cases. The maxima of the VTL from the slab to the tunnel invert in Cases 2, 4, and 5 were 42.4, 44.2, and 46.2 dB respectively, which shows that the smaller was the total effective spring stiffness, the greater was the VTL in the frequency range from 5 to 16 Hz.

Fig. 9 illustrates the vertical IL values on the tunnel invert (T4) and the tunnel apex (T6). Above 9 Hz, the vertical IL values were positive, which shows that vibrations can be attenuated by means of the FST. Vibration isolation efficiency in Case 2 was not as good as those in Cases 4 and 5, because the total effective spring stiffness was greater in Case 2; and the maximum of the vertical IL values was about 25 dB at around 12 Hz. At around the resonance frequencies in Cases 2, 4, and 5, the vertical IL values were negative, which indicates that vibrations can be amplified by using the FST.

Fig. 10 gives the vertical TCs from the slab to the tunnel invert and the tunnel apex. The vertical TC values in Case 1 were obviously the highest of all the

cases, and they became smaller and invariable in Cases 2, 4, and 5. The values varied moderately between frequencies of 5 and 16 Hz in all cases with isolation measures. For Case 1, the vertical TC values from the slab to the tunnel invert and the tunnel apex ranged between 0.012 and 0.028, while for Cases 2, 4, and 5, they ranged between 0 and 0.01.

3.3 Response on the ground surface

Fig. 11 shows the vertical and horizontal VALs at S1, S2, S3, S4, and S5 on the ground surface for different cases. Generally, the vertical response tended to be greater than the horizontal response; the maxima of the vertical and horizontal responses in Cases 1, 2, 4, and 5 appeared at about 12, 7, 6, and 6 Hz respectively. Due to the installation of steel springs, the vertical and horizontal responses on the ground surface declined markedly at frequencies above 9 Hz. In general, at frequencies greater than 7 Hz, Case 2 showed the greatest vertical response on the ground surface due to the installation of steel springs, and Case 5 the smallest; however, the variation in the horizontal responses due to the springs showed a different pattern at each position.

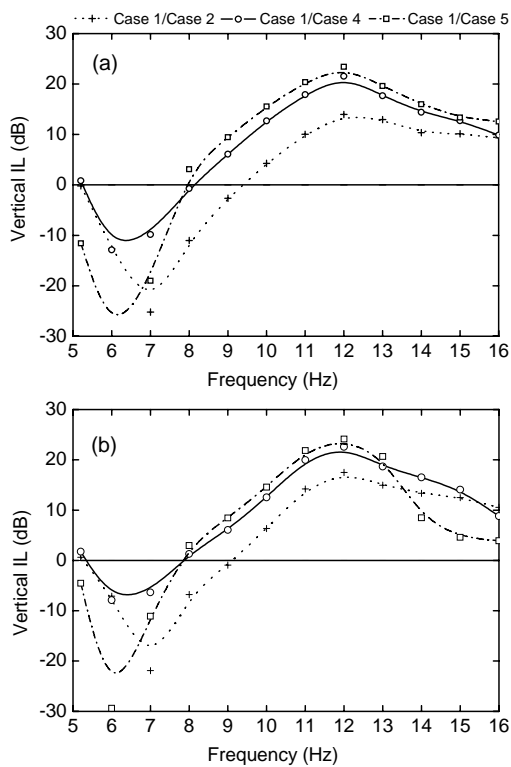


Fig. 9 Vertical insertion loss (IL) values at the tunnel invert T4 (a) and apex T6 (b)

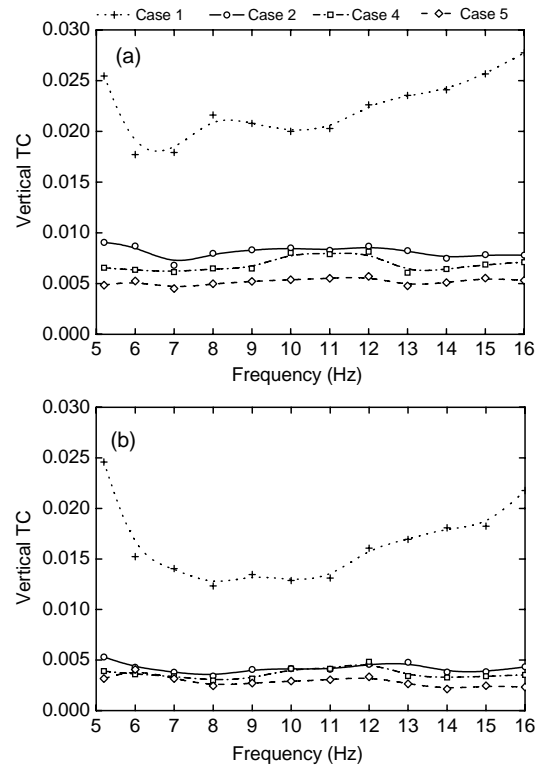


Fig. 10 Vertical transmission coefficients (TCs) from the slab to the tunnel invert T4 (a) and apex T6 (b)

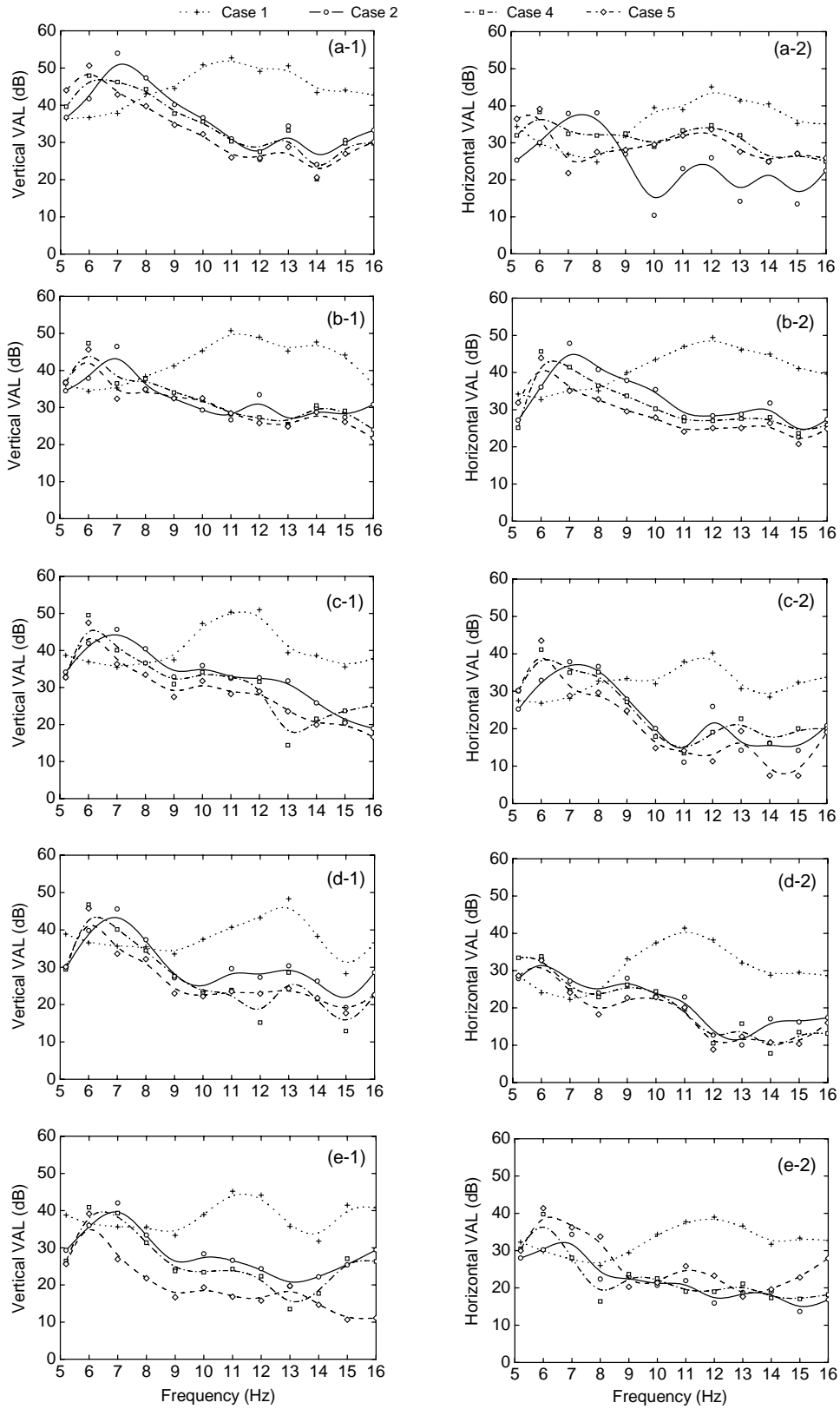


Fig. 11 Vertical (left) and horizontal (right) vibration acceleration levels (VALs) for different cases at different positions (a) S1; (b) S2; (c) S3; (d) S4; (e) S5

An important question is how the horizontal distance affects the variation in VALs. Fig. 12 shows the vertical and horizontal VALs as a function of the horizontal distance from the track at different frequencies in different cases. For Case 1, the vertical component changed moderately with distance at frequencies below 10 Hz, but reduced slightly with

distance at frequencies above 10 Hz; the horizontal component showed comparatively large variation within 40 m, and there was an amplification zone at around 20 m. For Cases 2, 4, and 5, the vertical component attenuated with distance overall; the horizontal component undulated with distance, and in general, there was also an amplification zone at about 20 m.

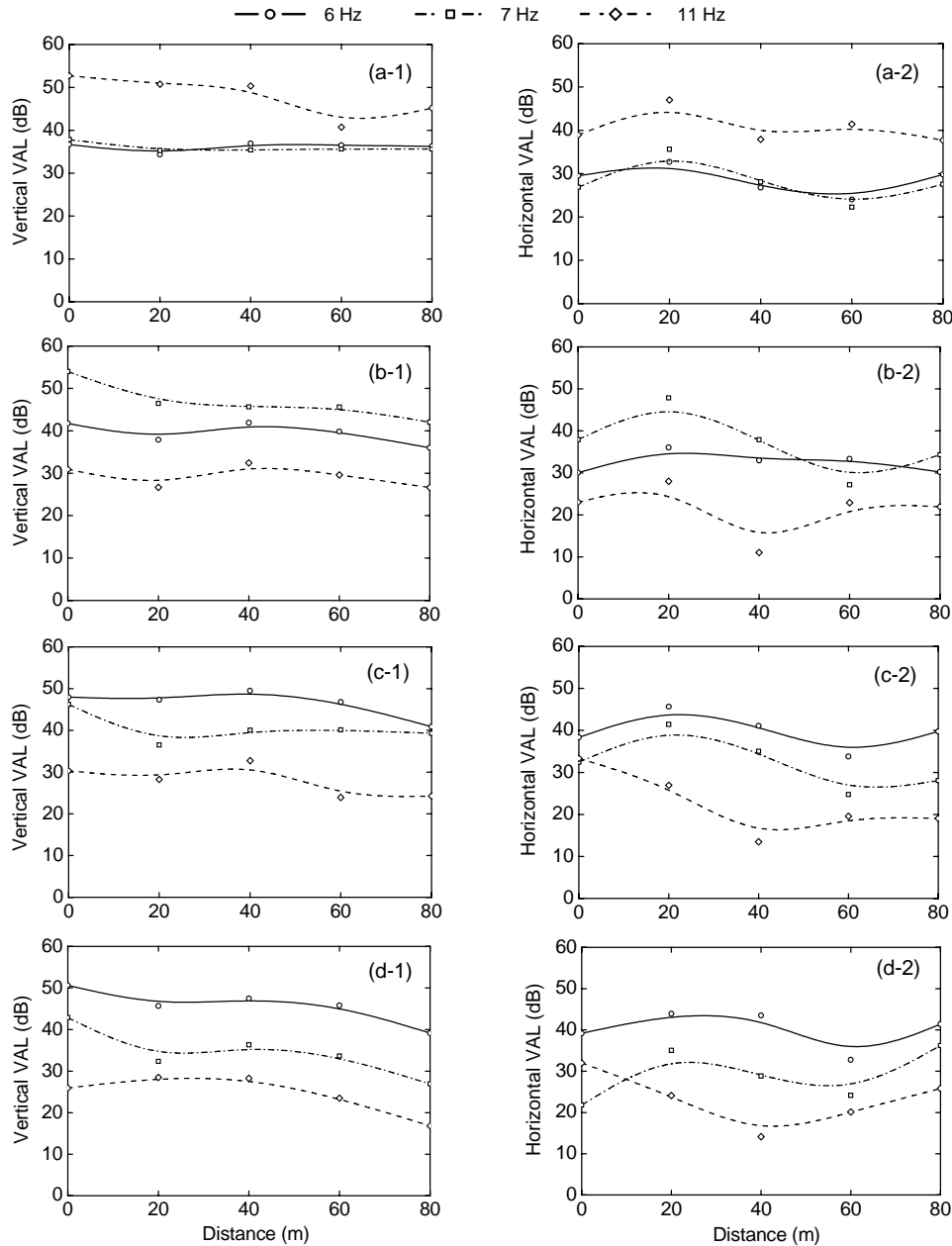


Fig. 12 Vertical (left) and horizontal (right) vibration acceleration levels (VALs) as a function of the distance from the track at different frequencies in different cases
 (a) Case 1; (b) Case 2; (c) Case 4; (d) Case 5

Fig. 13 shows the vertical and horizontal IL values at S1, S3, and S5 on the ground surface. At frequencies greater than 9 Hz, the vertical and horizontal responses were both positive, which shows that vibrations can be attenuated by using the FST. Vibration isolation efficiency reached up to 30 dB in the vertical direction and 25 dB in the horizontal direction. For the vertical response, above 9 Hz, vibration isolation performance in Case 5 was better than those in Cases 2 and 4 at distances between 0 and 80 m. For the horizontal response, above 9 Hz, vibration isolation efficiency in Case 2 was the best at 0 m, but decreased at 40 and 80 m; at 80 m, vibration isolation efficiency in Case 5 was worse than those of other cases, which shows that the reduction in the total effective spring stiffness was of no avail in attenuating

low frequency vibrations in the horizontal direction in the far field.

How do the soil layers attenuate low frequency vibrations? Vibrations on the tunnel invert were considered as an input, and the responses on the ground surface at different horizontal distances were regarded as some outputs. The vertical TCs from the tunnel invert to the ground surface were obtained in all cases, and were then averaged. Fig. 14 sums up the vertical TCs from the tunnel invert to the ground surface. With increasing distance, in general, the TCs decreased. The TC values from the tunnel invert to the ground surface ranged between 0 and 0.5. The TC values reduced slightly with the frequency, indicating that the soil layers could not easily dissipate low frequency vibrations.

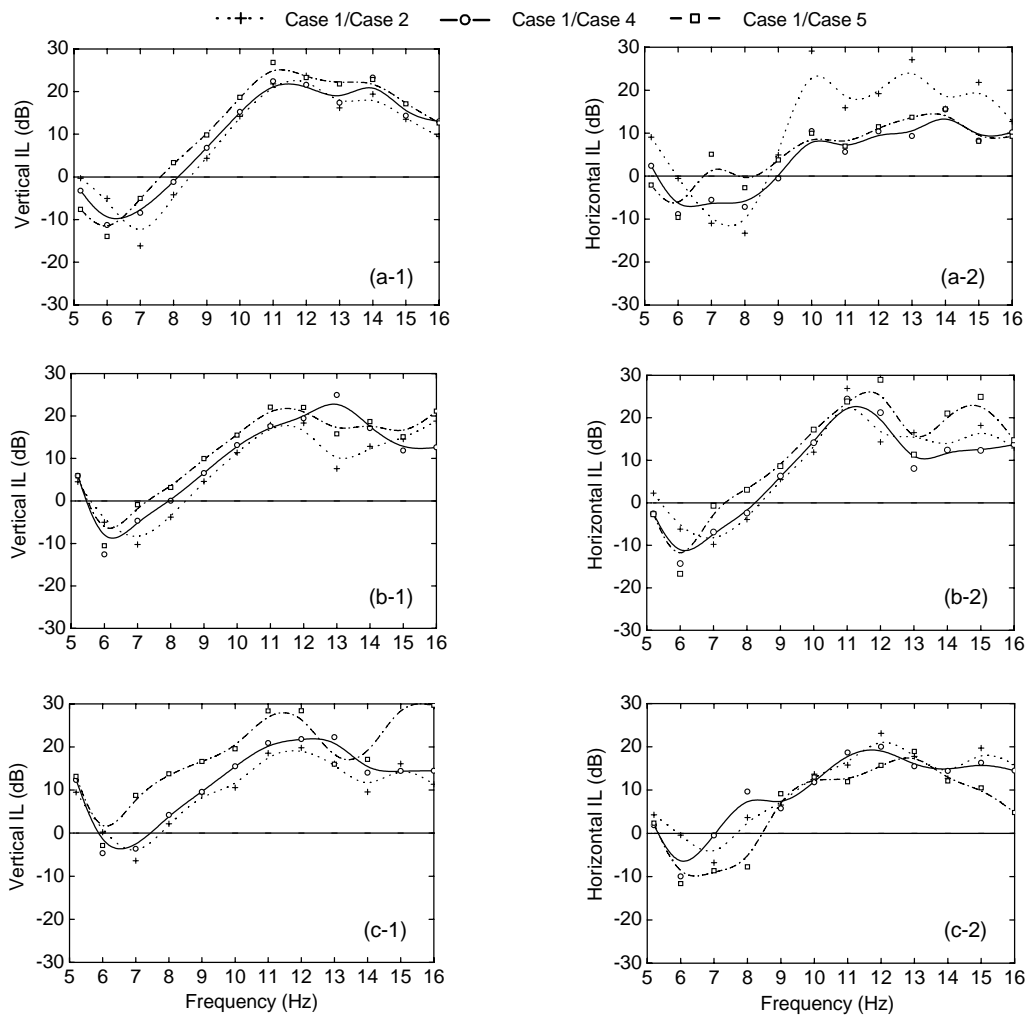


Fig. 13 Vertical (left) and horizontal (right) insertion loss (IL) values at different positions (a) S1; (b) S3; (c) S5

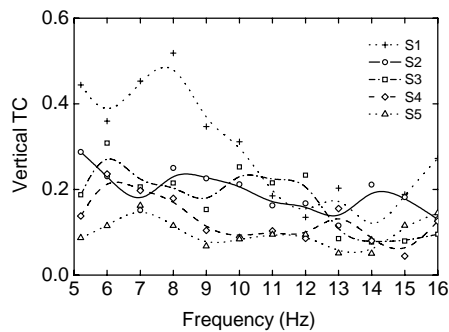


Fig. 14 Vertical transmission coefficients (TCs) from the tunnel invert to the ground surface

The low frequency vibration responses on the ground surface are dependent chiefly on the geologic characteristics of the soil surrounding the LTVAC. The stratigraphic section of the test site shows that there are seven main layers from top to bottom: fill material, fine sand, sandy silt, silty clay, gravel, silty clay, and gravel (Fig. 2), which is regarded as a typical stratum in Beijing. Therefore, low frequency vibration characteristics on the ground surface at the LTVAC can be applied to describe approximately the vibrations in other parts of Beijing.

3.4 Response in the building

Fig. 15 shows the vertical and horizontal VALs on different floors of the building in different cases. Generally, the horizontal response was greater than the vertical response, which is a different result from that on the ground surface. For the vertical response, the trends of VALs on different floors were the same for each case, and the VALs on all floors approximated each other. For the horizontal response, the VALs changed markedly with the frequency: below 9 Hz, the VALs on the 4th floor were the highest, while between 10 and 15 Hz they were the lowest.

Fig. 16 shows the vertical and horizontal VALs as a function of the floor number. In general, the vertical component varied moderately with the floor number and approximated on each floor. The horizontal component markedly increased with the floor number at frequencies below 10 Hz, and decreased at frequencies above 10 Hz.

Fig. 17 illustrates the vertical and horizontal IL values on the 2nd (B2) and 4th (B4) floors. Generally, vibrations in Cases 2, 4, and 5 could be attenuated at frequencies above 9 Hz, compared with those in

Case 1. However, they were amplified at around the natural frequencies of the FSTs. The maxima of vertical and horizontal responses were about 30 and 25 dB, respectively. As can be seen from the vertical and horizontal responses, above 9 Hz, vibration isolation efficiency in Case 2 was lower than those in the other cases.

The characteristics described above of low frequency vibrations in the building are dependent mainly on the construction of the Tunnel Center Building. The experimental results in this study can be used as a reference for predicting the vibrations of similar buildings. If a building had a different structure (foundation type, structure type, floor numbers, etc.), the vibration characteristics would change; therefore, it would be worth studying the low frequency vibrations in different buildings.

4 Conclusions

This paper summarizes important observations of low frequency vibration measurements performed in the Lab of Track Vibration Abatement and Control on the campus of Beijing Jiaotong University. The following conclusions can be drawn from the present analysis.

1. The basic frequencies of the floating slab track (FST) used in the tests were in the range between 6 and 7 Hz. When the spacing of steel springs was constant and their stiffness was reduced, or when the stiffness of steel springs was constant and the spacing of steel springs was lengthened, the basic frequency decreased.

2. The low frequency vibration transfer losses (VTLs) from the slab to the tunnel invert ranged between 29.7 and 46.2 dB. The greater was the total effective spring stiffness, the smaller was the VTL.

3. The low frequency vibration isolation efficiencies of the FST reached up to 30 dB. The maxima of vertical insertion loss (IL) in the tunnel, on the ground surface, and in the building were about 25, 30, and 30 dB, respectively. The maxima of horizontal IL on the ground surface and in the building were both 25 dB. At frequencies above 9 Hz, the low frequency vibrations were attenuated by the FST, while below 9 Hz, vibrations were amplified, especially, around the basic frequency.

4. The transmission coefficients (TCs) could be greatly reduced by the FST. The TCs from the slab to the tunnel without isolation measures ranged between 0.012 and 0.028. However, with the FST they ranged between 0 and 0.01.

5. The TCs of the soil at the test sites ranged between 0 and 0.5, and were slightly reduced with the

low frequency, indicating that the soil could not easily dissipate low frequency vibrations.

6. In the tests, the vertical low frequency vibrations played a leading role on the ground surface, compared with the horizontal ones. The vertical low frequency vibrations attenuated with the horizontal distance to the track; the horizontal low frequency

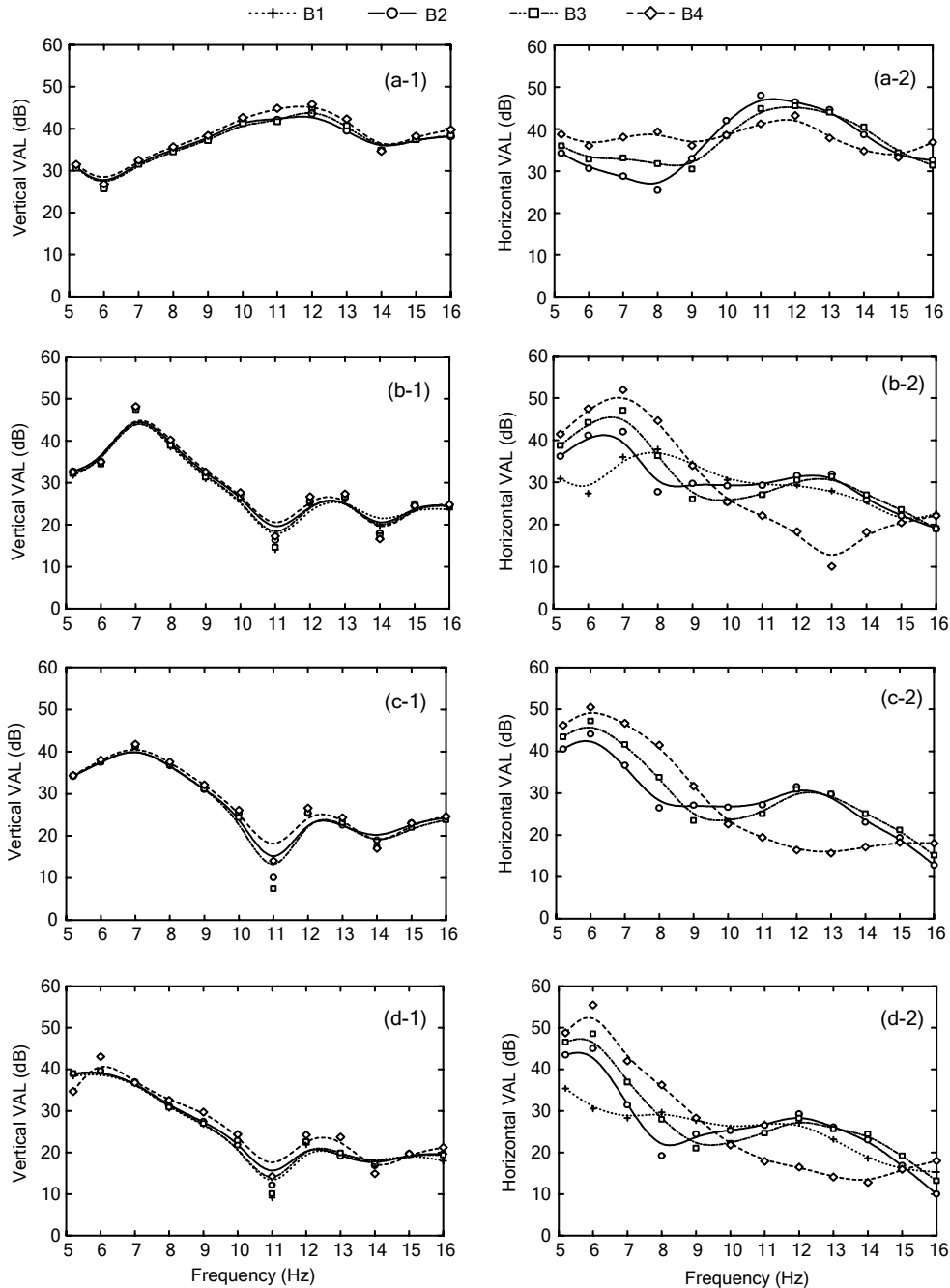


Fig. 15 Vertical (left) and horizontal (right) vibration acceleration levels (VALs) on different floors in different cases (a) Case 1; (b) Case 2; (c) Case 4; (d) Case 5

vibrations undulated with the distance and became amplified within 40 m of the track. There was an amplification zone at around 20 m.

7. In the tests, the horizontal low frequency vibrations played a primary role in the vicinity of the building, rather than the vertical vibrations. The

vertical low frequency vibrations varied moderately with the floor number and approximated on each floor; the horizontal low frequency vibrations markedly increased with the floor number at frequencies below 10 Hz, but decreased at frequencies above 10 Hz.

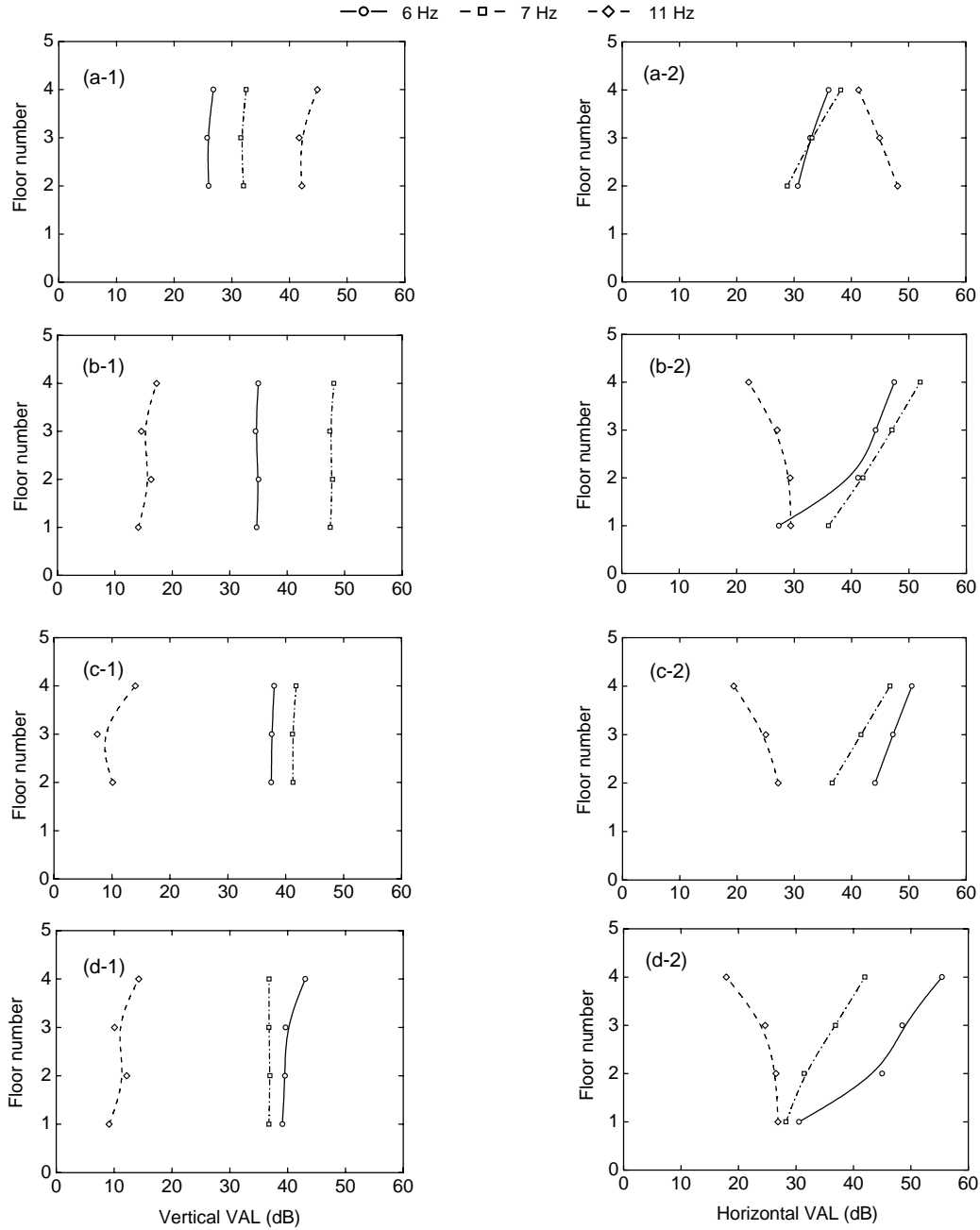


Fig. 16 Vertical (left) and horizontal (right) vibration acceleration levels (VALs) as a function of the floor number at different frequencies in different cases

(a) Case 1; (b) Case 2; (c) Case 4; (d) Case 5

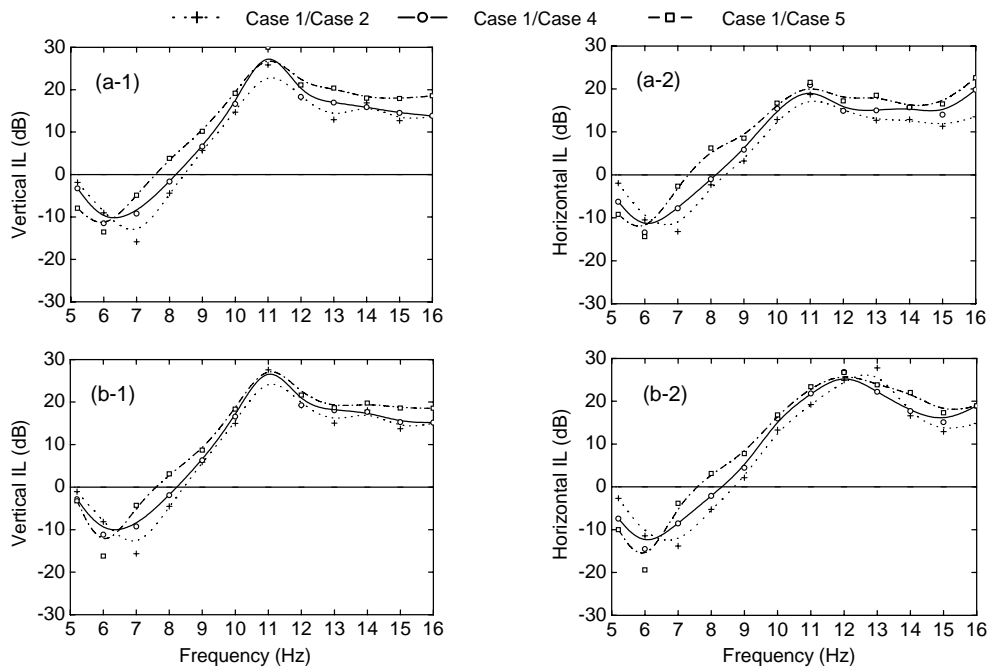


Fig. 17 Vertical (left) and horizontal (right) insertion loss (IL) values at different positions
(a) B2; (b) B4

References

- Cui, F., Chew, C.H., 2000. The effectiveness of floating slab track system—Part I. Receptance methods. *Applied Acoustics*, **61**(4):441-453. [doi:10.1016/S0003-682X(00)00014-1]
- Degrande, G., Schevenels, M., Chatterjee, P., van de Velde, W., Hölscher, P., Hopman, V., Wang, A., Dadjah, N., 2006. Vibrations due to a test train at variable speeds in a deep bored tunnel embedded in London clay. *Journal of Sound and Vibration*, **293**(3-5):626-644. [doi:10.1016/j.jsv.2005.08.039]
- Ding, D.Y., Liu, W.N., Zhang, B.C., Sun, X.J., 2008a. Modal analysis on the floating slab track. *Journal of the China Railway Society*, **30**(3):61-64 (in Chinese).
- Ding, D.Y., Gupta, S., Lombaert, G., Liu, W.N., Degrande, G., 2008b. The Prediction of Vibrations Induced by Underground Railway Traffic on Line 8 of Beijing Metro. Bilateral Project BIL/07/07, Report BWM-2008-22, K. U. Leuven, Belgium and Beijing Jiaotong University, China.
- Ding, D.Y., Gupta, S., Lombaert, G., Liu, W.N., Degrande, G., 2009. The Prediction of Vibrations Induced by Underground Railway Traffic on Line 15 of Beijing Metro. Bilateral Project BIL/07/07, Report BWM-2009-25, K. U. Leuven, Belgium and Beijing Jiaotong University, China.
- Ding, D.Y., Gupta, S., Liu, W.N., Lombaert, G., Degrande, G., 2010. Prediction of vibrations induced by trains on line 8 of Beijing metro. *Journal of Zhejiang University-SCIENCE A (Applied Physics & Engineering)*, **11**(4): 280-293. [doi:10.1631/jzus.A0900304]
- Gupta, S., Liu, W.F., Degrande, G., Lombaert, G., Liu, W.N., 2008. Prediction of vibrations induced by underground railway traffic in Beijing. *Journal of Sound and Vibration*, **310**(3):608-630. [doi:10.1016/j.jsv.2007.07.016]
- Kuo, C.M., Huang, C.H., Chen, Y.Y., 2008. Vibration characteristics of floating slab track. *Journal of Sound and Vibration*, **317**(3-5):1017-1034. [doi:10.1016/j.jsv.2008.03.051]
- Liu, W.N., Zhang, H.R., Li, R.D., 2005a. Report on Environmental Vibration Measurements in Beijing Metro Line 1. Report 2005-12, Beijing Jiaotong University, Beijing, China (in Chinese).
- Liu, W.N., Ding, D.Y., Sun, X.J., Liu, W.F., 2005b. Study on Special Vibration Reduction Measures in Beijing Metro Line 4. Report 2005-08, Beijing Jiaotong University, Beijing, China (in Chinese).
- Liu, W.F., Gupta, S., Degrande, G., Liu, W.N., 2006. Numerical Modelling of Vibrations Induced by Underground Railway Traffic on Metro Line 4 in Beijing. Bilateral Project BIL/04/17, Report BWM-2006-08, K. U. Leuven, Belgium and Beijing Jiaotong University, China.
- Lombaert, G., Degrande, G., Vanhauwere, B., Vandeborghet, B., François, S., 2006. The control of ground-borne vibrations from railway traffic by means of continuous floating slabs. *Journal of Sound and Vibration*, **297**(3-5): 946-961. [doi:10.1016/j.jsv.2006.05.013]
- London Transport Office of the Scientific Adviser, 1982. Vibration Measurement at Baker Street (Jubilee Line). London, UK.

- Nelson, J.T., 1996. Recent developments in ground-borne noise and vibration control. *Journal of Sound and Vibration*, **193**(1):367-376. [doi:10.1006/jsvi.1996.0277]
- Pan, C.H., Xie, Z.G., 1990. Measurement and analysis of vibrations caused by passing trains in subway running tunnel. *China Civil Engineering Journal*, **23**(2):21-28 (in Chinese).
- Ruker, W., 1977. Measurement and Evaluation of Random Vibrations. Proceedings of DMSR 77, Karlsruhe, Germany, **1**:407-421.
- Saurenman, H., Phillips, J., 2006. In-service tests of the effectiveness of vibration control measures on the BART rail transit system. *Journal of Sound and Vibration*, **293**(3-5): 888-900. [doi:10.1016/j.jsv.2005.08.045]
- Sun, X.J., Liu, W.N., Zhang, B.C., 2005. Applications of floating slab track framework for vibration and noise control in urban rail traffic. *China Safety Science Journal*, **15**(8):65-69 (in Chinese).
- Wilson, G.P., Saurenman, H.J., Nelson, J.T., 1983. Control of ground-borne noise and vibration. *Journal of Sound and Vibration*, **87**(2):339-350. [doi:10.1016/0022-460X(83)90573-4]
- Wolf, S., 2003. Potential low frequency ground vibration (<6.3 Hz) impacts from underground LRT operations. *Journal of Sound and Vibration*, **267**(3):651-661. [doi:10.1016/S0022-460X(03)00730-2]
- Zhang, B.C., Xu, Z.X., 2002. Applications of the steel spring floating track bed for vibration and noise control in urban rail traffic. *China Railway Science*, **23**(3):68-71 (in Chinese).

Information on JZUS(A/B/C)

(<http://www.zju.edu.cn/jzus>)

In 2010, we have updated the website and opened a few active topics:

- **The top 10 cited papers in parts A, B, C;**
 - **The newest cited papers in parts A, B, C;**
 - **The top 10 DOIs monthly;**
 - **The 10 most recently commented papers in parts A, B, C.**
- (Welcome your comment and opinion!)**

We also list the International Reviewers to express our deep appreciation and Crosscheck information etc.

If you would like to allot a little time to opening <http://www.zju.edu.cn/jzus>, you will find more interesting information. Many thanks for your interest in our journals' publishing change and development in the past, present and future!

Welcome you to comment on what you would like to discuss. And also welcome your interesting/high quality paper to JZUS(A/B/C) soon.

Top 10 cited A B
Optimal choice of parameter...
How to realize a negative r...
Three-dimensional analysis ...
THE POLYMERIZATION OF METHY...
Hybrid discrete particle sw...
more
Newest cited A B C
AN ULTRAHIGH VACUUM CHEMICA...
RESEARCH ON THE METHODS OF ...
STUDY OF THE EFFECTIVENESS ...
Sliding mode identifier for...
Buckling of un-stiffened cy...
more
Top 10 DOIs Monthly
Continuum damage mechanics ...
A numerical analysis to the...
Model-based testing with UM...
Nonlinear identification of...
Global nutrient profiling b...
more
Newest 10 comments
Robust design of static syn...
Acute phase reactants, chal...
Optimized simulated anneali...
Advanced aerostatic analysi...
Global nutrient profiling b...
more